Article

The strand-specific regulation of miR-155-3p in response to lipopolysaccharide and interleukin-10 stimulation requires FUBP1 protein

Jeff S. J. Yoon [1, 2, 3], Abdulwadood Baksh [3], Thomas C. Chamberlain [1, 2, 3, &] and Alice L-F Mui [1, 2, 3, &*]

[1] Immunity and Infection Research Centre, Vancouver Coastal Health Research Institute, Vancouver, Canada
[2] Department of Surgery, University of British Columbia, Vancouver, Canada
[3] Department of Biochemistry and Molecular Biology, University of British Columbia, Vancouver, Canada
[&] TC and ALFM are co-senior authors
[*] Correspondence: alice.mui@ubc.ca

Abstract: The microRNA-155 (miR-155) promotes inflammatory responses in macrophages. Activating macrophages with lipopolysaccharide (LPS) elevates miR-155, while the anti-inflammatory cytokine interleukin-10 (IL10) reduces miR-155 levels. MiR-155 exists in two forms, miR-155-5p and miR-155-3p, produced from the precursor of miR-155 (pre-miR-155). LPS stimulation of macrophages results first in elevation of miR-155-3p levels, followed by increases miR-155-5p. We previously identified the CELF2 protein to interact with pre-miR-155 and impair miR-155-5p expression. We now show that CELF2 only regulates the miR-155-5p expression and that another protein called FUBP1 controls miR-155-3p levels in response to LPS and IL10.

Keywords: miR-155, FUBP1, strand selection, interleukin-10

1. Introduction

MicroRNAs (miRNAs) are short regulatory non-coding RNAs that post-transcriptionally regulate the expression of genes through sequence-specific targeting of mRNA [1]. Initially discovered as involved in the cellular development of larval *Caenorhabditis elegans*, miRNAs have now been shown to regulate many genes in mammalian cells [2,3], including the host immune cell response to pathogens. For example, an innate immune cell called a macrophage [4] becomes activated to produce inflammatory cytokines by exposure to bacterial cell wall components such as lipopolysaccharide (LPS) to help eliminate the pathogen [4-8]. O'Connell *et al.* identified miRNA-155 (miR-155) as a key miRNA induced in the inflammatory response [7] and required for macrophage expression of the inflammatory cytokine tumor necrosis factor-alpha (TNFα) [7].

Macrophage activation plays an important part in the host's defense against pathogens [4,6]. However, persistent macrophage activation can become harmful, leading to inflammatory diseases, cardiovascular diseases, atherosclerosis, Alzheimer's disease, and cancers [9-11]. Consequently, activated macrophages also release anti-inflammatory cytokines, namely interleukin-10 (IL10), to attenuate the pro-inflammatory effects of macrophages activated by LPS [12]. IL10 is a pleiotropic cytokine originally characterized as a cytokine synthesis inhibitory factor produced by murine Th_2 T-cells to prevent cytokine production by murine Th_1 T-cells [12], but deactivating activated macrophages is it's major *in vivo* function [13]. IL10 receptor (IL10R) signaling uses both the Signal Transducer and Activator of Transcription 3 (STAT3) [14-16] and Src Homology 2 domain-containing Inositol-5 Phosphatase 1 (SHIP1)-dependent [14,17,18] pathways to deactivate macrophages [15,17-20]. We previously reported that SHIP1 could form a complex with STAT3 (SHIP1:STAT3) in response to IL10R signaling or through the exposure of cells to small molecules that bind to induce a conformational change in SHIP1 [14]. The formation of

Preprints (www.preprints.org) | NOT PEER-REVIEWED | Posted: 15 November 2021 doi:10.20944/preprints202111.0272.v1

the SHIP1:STAT3 complex is sufficient to inhibit macrophage production of TNFα. We also showed that IL10 inhibition of miR-155-5p required SHIP1 and STAT3 [18].

The MIR155HG locus encodes MiR-155, and the primary transcript of miR-155 (**pri-miR-155**) undergoes Drosha-mediated cleavage to the precursor of miR-155 (**pre-miR-155**) [21]. Pre-miR-155 can be processed into two different forms, miR-155-5p and miR-155-3p [22], depending on which strand from the pre-miR-155 is selected. This strand becomes loaded onto the RNA-induced silencing complex (RISC) and forms the guide strand while the other is degraded [23]. The 5p and 3p strands have different seed sequences and thus target different mRNAs [24]. We previously showed that IL10 inhibits the maturation of pre-miR-155 into mature miR-155-5p [18]. We then used mass spectrometry to identify proteins that bind to pre-miR-155 to characterize the mechanism by which IL10R signaling inhibits pre-miR-155 maturation [25]. We found CUGBP Elav-Like Family member 2 (CELF2) protein associates with pre-miR-155 in an IL10 dependent manner, and deletion of CELF2 enhanced LPS-induced expression of miR-155-5p suggesting that CELF2's role is to inhibit miR-155-5p expression. Recently, Simmonds *et al.* showed that LPS stimulation leads to the early expression of miR-155-3p, followed by miR-155-5p [26]. Thus, in the current study, we investigated whether CELF2 or another protein called Far Upstream element Binding Protein 1 (FUBP1), which we also observed to bind to pre-miR-155 [25], might be involved in regulating miR-155-3p levels.

FUBP1 belongs to a family of RNA-binding proteins, including the KH-type Splicing Regulatory Protein (KSRP) [27]. Studies into the mechanism of pre-miR-155 maturation have previously implicated KSRP in controlling miR-155-p expression in macrophages [28,29] and dendritic cells [30]. Ruggiero *et al.* reported that pre-miR-155 co-immunoprecipitated with KSRP and KSRP depletion impaired the expression of mature miR-155-5p while simultaneously causing the accumulation of pri-miR-155 and pre-miR-155 [28]. KSRP, also known as Far Upstream element Binding Protein 2 (FUBP2), binds to the terminal loop of pre-miR-155 via four distinct hnRNPK-Homology (KH) domains and promotes its maturation [28,31,32].

We now describe the role of FUBP1 in the control of miR-155-3p expression. First, we show that FUBP1 increases its association with pre-miR-155 in response to LPS and IL10. Second, we examined the role of FUBP1 in macrophage function by creating FUBP1 deficient cells using CRISPR-Cas9-mediated gene targeting. We found that in LPS stimulated macrophages, IL10 inhibition of TNFα requires FUBP1. Interestingly, FUBP1 affects the production of the two alternative strands of miR-155, miR-155-5p, and miR-155-3p oppositely: FUBP1 promotes miR-155-3p expression but inhibits miR-155-5p. Finally, we show that FUBP1's KH domain 3 mediates FUBP1 binding to pre-miR-155, suggesting an important new role for FUBP1 in controlling miR-155 biogenesis affecting the inflammatory response of macrophages.

2. Results

2.1. Interleukin-10 induces association of FUBP1 to pre-miR-155

We and others have shown that IL10 inhibits LPS-induced miR-155-p expression in macrophage cells *[18,25]*. We further showed that IL10 inhibits the maturation of pre-miR-155 to mature miR-155- 5p *[18]* and that the RNA binding protein CELF2 contributes to the process *[25]*. However, our mass spectrometry-based examination pre-miR-155 associated proteins had also identified FUBP1 as another protein that might interact with pre-miR-155 in an LPS and IL10 dependent manner *[25]*.

To follow up on the mass spectrometry data, we analyzed pre-miR-155 pull-down samples for the presence of FUBP1 protein. The amount of FUBP1 observed in cell lysates

Preprints (www.preprints.org) | NOT PEER-REVIEWED | Posted: 15 November 2021 doi:10.20944/preprints202111.0272.v1

remained constant regardless of whether the cells were stimulated or not, suggesting that FUBP2 expression levels do not change in response to stimulations. Instead, it is the association of FUBP1 with pre-miR-155 that changes. FUBP1 in the pull-down was quantified and normalized to the total FUBP1 in cell lysates. As seen in **Figure 1**, LPS treatment of cells increased the amount FUBP1 associated with pre-miR-155 is with no additional effect of IL10 stimulation.

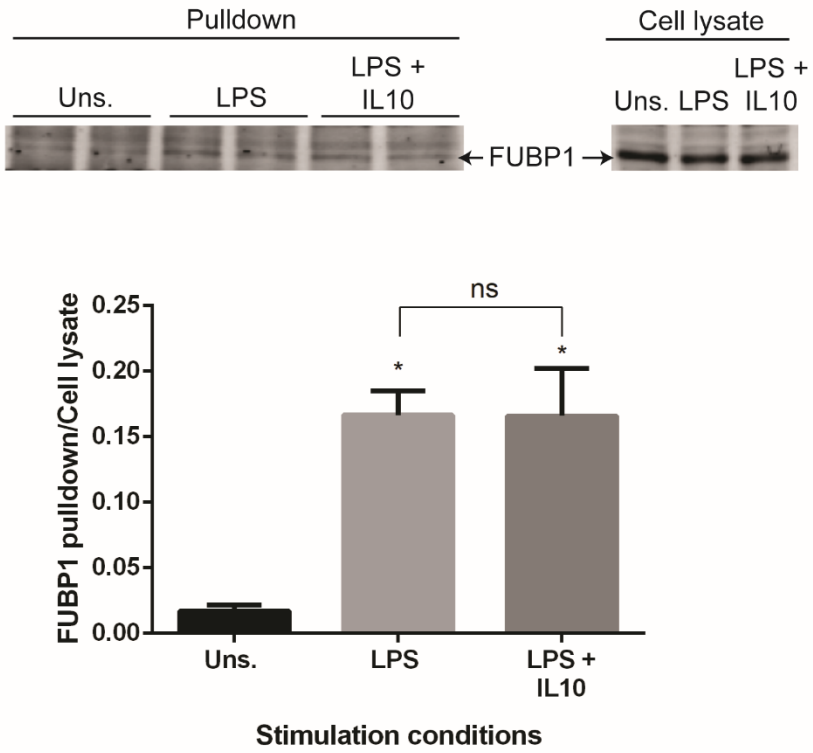

Figure 1. Increased interaction of FUBP1 protein with pre-miR-155 in response to LPS stimulation.

RAW264.7 cells were transfected with biotinylated pre-miR-155 oligonucleotide and stimulated with LPS ± IL10 for 2 hours before collecting the pull-down samples. Expression levels of FUBP1 protein interacting with pre-miR-155 oligonucleotide were determined by immunoblotting. The graph shows the FUBP1 band intensities in the pull-down sample normalized to the FUBP1 protein in total cell lysate. The significance in the difference between the LPS ± IL10 stimulations to unstimulated sample or comparison indicated was calculated by One-Way ANOVA with Tukey's correction. * $p < 0.05$, ns = not significant.

2.2. FUBP1 deficiency differentially regulates miR-155-5p and miR-155-3p expression

IL10 inhibits TNFα production and miR-155-p induction in LPS-stimulated macrophages *[18,25,28]*. To investigate the role of FUBP1 in LPS and IL10 action in these pathways, we used CRISPR-Cas9-mediated targeting to knockdown (KD) FUBP1 in RAW264.7 cells. As illustrated in **Figure 2a**, the FUBP1 KD cells express significantly less FUBP1 protein than the non-target cells.

Preprints (www.preprints.org) | NOT PEER-REVIEWED | Posted: 15 November 2021 doi:10.20944/preprints202111.0272.v1

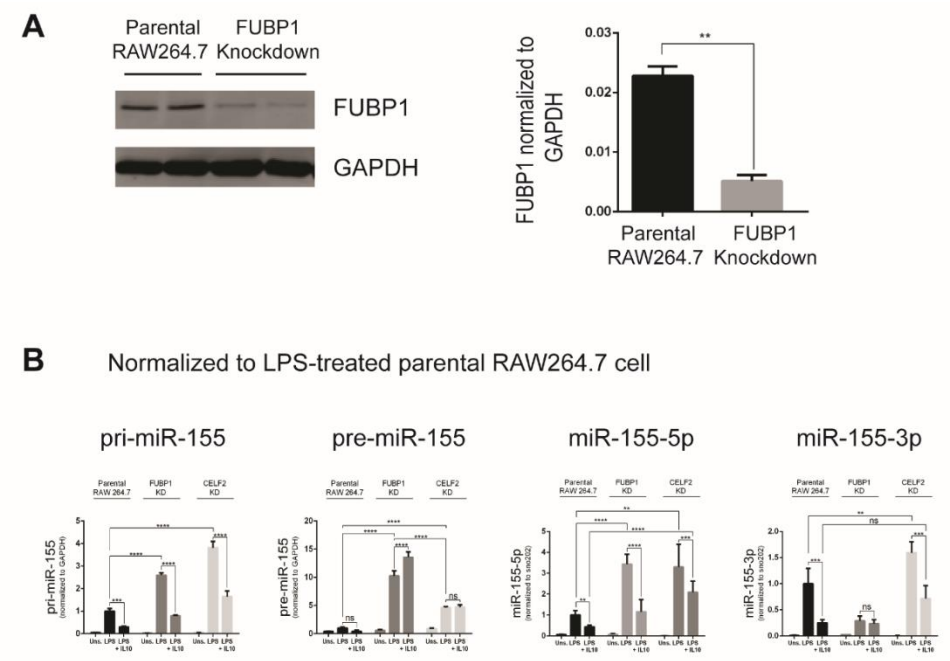

Figure 2. FUBP1 deficiency alters the expression of miR-155-5p and miR-155-3p in response to LPS ± IL10

RAW264.7/Cas9 cells transduced with FUBP1 sgRNA were treated with 2 μg/mL of doxycycline to induce knockdown of FUBP1 protein. (a) FUBP1 protein expression was determined by immunoblotting. Data plotted represents FUBP1 protein band intensity normalized to GAPDH (unpaired Student's *t*-test). (b) FUBP1 KD, CELF2 KD, or the parental RAW264.7 cells were stimulated with 1 ng/mL of LPS ± 1 ng/mL of IL10 for 4 hours before total RNA extraction. The expression level of pr-miR-155, pre-miR-155, miR-155-5p, and miR-155-3p was determined by qPCR and normalized to GAPDH or snoRNA202 levels. Data plotted represents the expression level of pri-miR-155, pre-miR-155, miR-155-5p, and miR-155-3p normalized to the LPS-stimulated sample of parental RAW264.7 cells. Two-Way ANOVA determined the comparison between the stimulations indicated (with braces) with Tukey's correction. **** $p < 0.0001$, *** $p < 0.001$, ** $p < 0.01$, * $p < 0.05$, ns = not significant.

After confirming the reduction of FUBP1 protein in the FUBP1 KD cells, we stimulated the parental RAW264.7, FUBP1 KD, and CELF2 KD cells with LPS ± IL10 for 4 hours, isolated RNA, and quantified the levels of pri-miR-155, pre-miR-155, miR-155-5p, and miR-155-3p via qPCR. The data were all normalized to the LPS-stimulated sample of the parental RAW264.7 cells. **Figure 2b** shows that knocking down CELF2 does not alter the basal (unstimulated) expression of pri-miR-155, pre-miR-155, miR-155-5p and miR-155-3p. However, the LPS-stimulated levels of all four increased in CELF2 KD cells, consistent with our previous finding that CELF2 is a negative regulator of miR-155-5p expression [25]. Also, as we previously reported, IL10 inhibition of miR-155-5p is impaired in CELF2 KD cells [25]. However, we now show that IL10 inhibition of miR-155-3p is normal in the CELF2 KD cells (**Figure 2b**, rightmost panel).

Knocking down FUBP1 also does not affect the basal level of the pri-miR-155, pre-miR-155, miR-155-5p, and miR-155-3p in unstimulated cells (**Figure 2b**). As observed in CELF2 KD cells, LPS-stimulated levels of pri-miR-155, pre-miR-155, and miR-155-5p are increased in the FUBP1 KD compared to the parental RAW264.7 cells. However, unlike CELF2 KD, LPS-stimulated miR-155-3p levels are decreased. Furthermore, IL10 can inhibit LPS-stimulated miR-155-5p but not miR-155-3p expression in FUBP1 KD cells. These observations suggest that FUBP1 may participate miR-155- strand selection [33] in LPS and IL10 treated macrophage cells.

Preprints (www.preprints.org) | NOT PEER-REVIEWED | Posted: 15 November 2021 doi:10.20944/preprints202111.0272.v1

Previous studies report that miR-155 deficiency results in increased LPS-induced inflammatory cytokine production [25,28]. Therefore, we examined IL10's action on TNFα production in FUBP1 KD cells. Cells were stimulated with LPS ± 0.5 ng/mL or 10 ng/mL IL10 for 1 hour, and TNFα levels in the supernatant were quantified by ELISA. **Figure 3** shows that in parental RAW264.7 cells, IL10 inhibits LPS-induced TNFα expression in a dose-dependent manner. However, in FUBP1 KD cells, IL10 could not decrease LPS-induced TNFα levels at either concentration of IL10 tested. This impairment of IL10 action suggests IL10R signaling requires FUBP1 for IL10 inhibition of LPS-induced TNFα, perhaps by reducing the level of miR-155-3p in response to IL10.

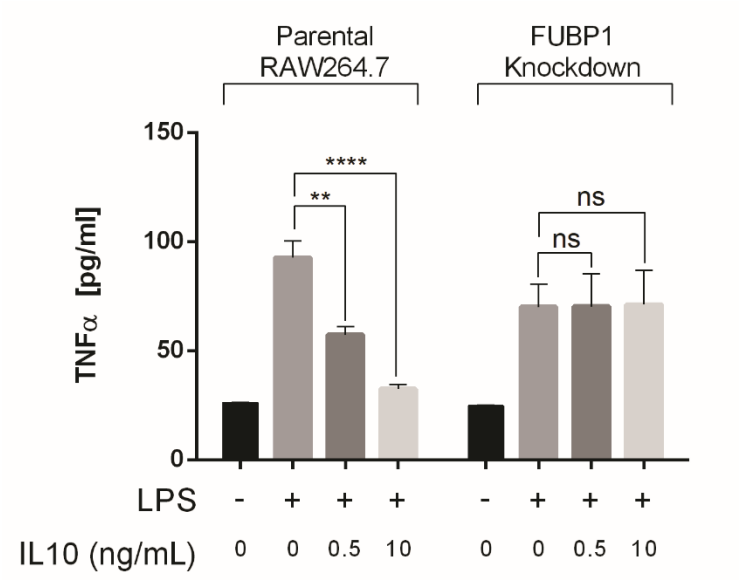

Figure 3. FUBP1 deficiency alters the expression of TNFα in response to LPS ± IL10

FUBP1 KD cells were stimulated with 1 ng/mL LPS ± indicated concentration of IL10 for 1 hour before collecting the cell culture supernatant. The level of TNFα in the supernatants was determined by ELISA. (Two-Way ANOVA with Tukey's correction. *** $p < 0.001$, ** $p < 0.01$, ns = not significant).

2.3. SHIP1 and STAT3 dependence of miR-155-5p and miR-155-3p expression

We have previously shown that IL10 requires SHIP1 and STAT3 to inhibit miR-155-5p production in LPS stimulated macrophages [17,18]. However, we had not examined the expression of the alternate miR-155 strand, miR-155-3p. Thus, we extracted peritoneal macrophages (perimacs) from SHIP1 or STAT3 wild type (WT) or knockout (KO) mice, rested the cells for 2 hours, stimulated the cells with LPS ± IL10 for 4 hours, isolated RNA, and quantified the levels of pri-miR-155, pre-miR-155, miR-155-5p and miR-155-3p.

Figure 4a shows the pri-miR-155, pre-miR-155, miR-155-5p and miR-155-3p expression in STAT3 WT and STAT3 KO cells at 4 hours after LPS ± IL10 stimulation. The qPCR gene expression data were normalized to the LPS-stimulated STAT3 WT sample to compare the expression in STAT3 WT and STAT3 KO cells. The basal levels of pri-miR-155, pre-miR-155, miR-155-5p, and miR-155-3p are equal in unstimulated STAT3 WT and KO perimacs (**Figure 4a**). The expression of LPS-stimulated miR-155-5p and miR-155-3p were also similar in STAT3 WT vs. STAT3 KO cells. However, the levels of LPS-stimulated pri-miR-155 and pre-miR-155 are increased in the STAT3 KO compared to the STAT3 WT cells. Thus, IL10 could not inhibit expression of pri-miR-155, pre-miR-155, miR-155-5p, or miR-155-3p in STAT3 KO cells and instead *increased* the level of miR-155-5p and miR-155-

Preprints (www.preprints.org) | NOT PEER-REVIEWED | Posted: 15 November 2021 doi:10.20944/preprints202111.0272.v1

3p in STAT3 KO cells. These effects of STAT3 KO on LPS and IL10 regulation of pri-miR-155, pre-miR-155, miR-155-5p, and miR-155-3p can also be seen when the qPCR gene expression data were normalized to each cell type's own LPS-stimulated sample (**Figure 4b**).

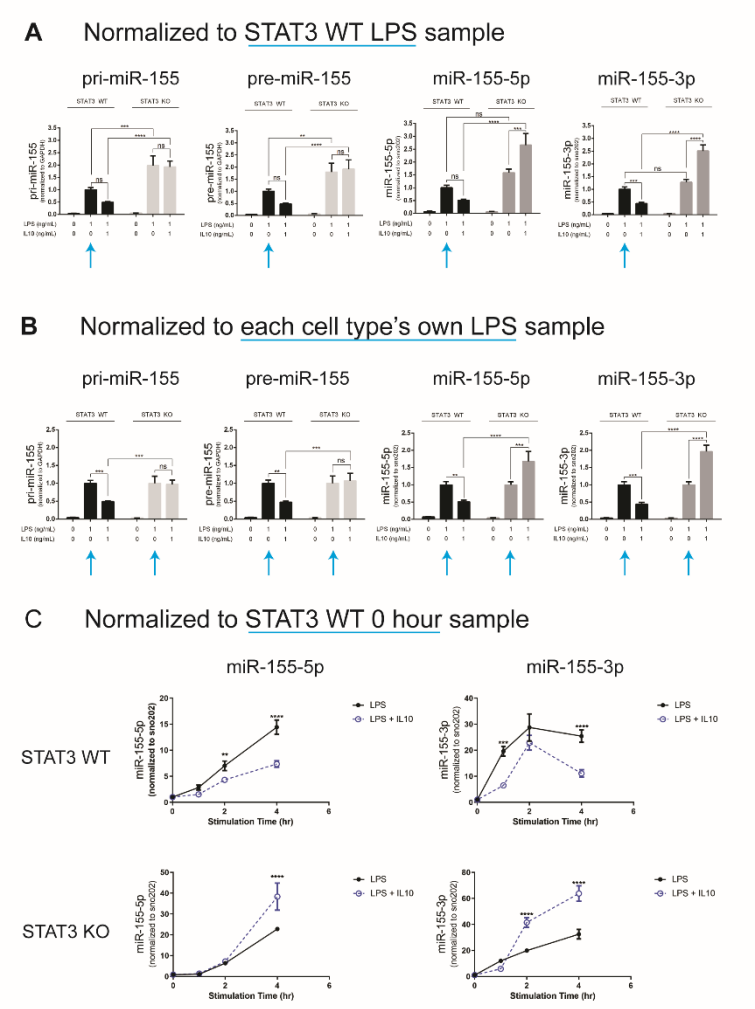

Figure 4. STAT3 dependence of miR-155-5p and miR-155-3p expression

Expression level in STAT3 WT and KO cells of pri-miR-155, pre-miR-155, miR-155-5p or miR-155-3p was determined by qPCR and normalized to GAPDH or snoRNA202 levels. (a) Data plotted to represent the RNA expression normalized to LPS-stimulated sample of the STAT3 WT. (b) The data in panel A replotted with RNA expression normalized to each cell's own LPS-stimulated sample. (c) Kinetics of miR-155-5p and miR-155-3p expression normalized to the STAT3 WT 0 hour sample. The significance of the difference in values (if any) between the LPS ± IL10 stimulated sample at the same time point was determined by Two-Way ANOVA with Tukey's correction. **** $p < 0.0001$, *** $p < 0.001$, ** $p < 0.01$, ns = not significant.

We then examined the kinetics of miR-155-5p and miR-155-3p expression (**Figure 4c**). In STAT3 WT cells stimulated with LPS, miR-155-3p rises rapidly with a peak at 2 hours, while miR-155-5p rises more slowly but is still rising at 4 hours. The presence of IL10 (LPS + IL10) reduced the levels of both miR-155-5p and miR-155-3p. These kinetics are similar to those observed by Simmonds *et al.* in human peripheral blood-derived macrophages [26]. In STAT3 KO cells stimulated with LPS, miR-155-3p levels also rise before miR-155-5p. Remarkably, the presence of IL10 (LPS + IL10) *enhanced* rather than inhibited the ex-

Preprints (www.preprints.org) | NOT PEER-REVIEWED | Posted: 15 November 2021 doi:10.20944/preprints202111.0272.v1

pression of both miR-155-5p and miR-155-3p. We did not look at longer time points because the effect of autocrine cytokines will contribute to gene expression at longer stimulation times.

We next examined the levels of pri-miR-155-, pre-miR-155, miR-155-5p, and miR-155-3p in SHIP1 WT and KO cells at 4 hours of stimulation. Perimacs were isolated from mice as described above. The **Figure 5a** data are normalized to the LPS-stimulated sample of the SHIP1 WT cell and show that SHIP1 deficiency leads to elevated basal (unstimulated) levels of pri-miR-155, pre-miR-155, miR-155-5p and miR-155-3p. Paradoxically, the LPS-stimulated expression of all four RNAs is decreased in the SHIP1 KO compared to the SHIP1 WT cells. To see if IL10 could inhibit the LPS-induced expression of the four RNAs in the SHIP1 KO cells and account for impaired LPS stimulation of the four RNAs, we normalized the RNA expression data to each cell's own LPS-stimulated sample. As **Figure 5b** shows, IL10 can inhibit LPS-induced pri-miR-155, pre-miR-155, and miR-155-5p in both SHIP1 WT and KO cells, but IL10 inhibition of miR-155-3p is impaired in the SHIP1 KO as compared to the SHIP1 WT cells. These observations suggest IL10 control miR-155-3p expression is more dependent on SHIP1 signaling than of miR-155-5p.

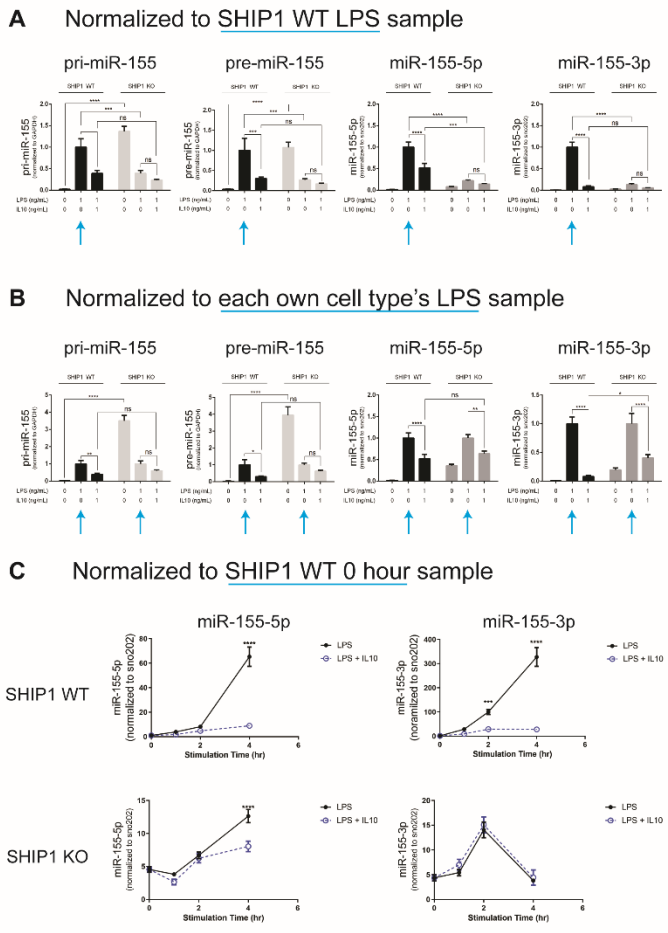

Figure 5. SHIP1 dependence of miR-155-5p and miR-155-3p expression

Expression level in SHIP1 WT and KO cells of pri-miR-155, pre-miR-155, miR-155-5p or miR-155-3p was determined by qPCR and normalized to GAPDH or snoRNA202 levels. (a) Data plotted to represent the RNA expression normalized to LPS-stimulated sample of the SHIP1 WT cell. (b) The data in panel A replotted with RNA expression normalized to each cell's own LPS-stimulated sample. (c) Kinetics of miR-155-5p and miR-155-3p expression with RNA normalized to the SHIP1 WT 0 hour sample. The significance of the difference in values (if any) in the LPS ± IL10 stimulated

 doi:10.20944/preprints202111.0272.v1

sample at the same time point was determined by Two-Way ANOVA with Tukey's correction. **** $p < 0.0001$, *** $p < 0.001$, ** $p < 0.01$, * $p < 0.05$, ns = not significant.

Figure 5c shows the kinetics of miR-155-5p and miR-155-3p expression in the SHIP1 WT and SHIP1 KO cells. In SHIP1 WT cells, miR-155-3p can be detected at 2 hours, which is earlier than miR-155-5p which is seen only at 4 hours. The kinetics of both miR-155-3p and miR-155-5p in the SHIP1 WT cells (**Figure 5c**) is slightly delayed compared to the STAT3 WT cells (**Figure 4c**). This difference might reflect the different genetic backgrounds of SHIP1 WT/KO (BALB/c) vs. STAT3 WT/KO mice (C57BL/6). IL10 could inhibit miR-155-5p in both SHIP1 WT and KO cells. However, IL10 inhibited miR-155-3p expression less well in SHIP1 KO as compared to SHIP1 WT cells.

2.4. FUBP1 interacts with pre-miR-155 via KH domain 3

Our data suggest that the regulation of miR-155-3p expression in response to LPS and IL10 is dependent on FUBP1. Previous studies have shown the RNA-binding protein KSRP interacts with pri-miR-155 and pre-miR-155 to regulate miR-155 expression [28,30]. In addition, Zhou *et al*. described KSRP as required for regulation of miR-155-5p; in KSRP deficient cells, miR-155-5p levels in response to LPS stimulation in dendritic cells are decreased, while miR-155-3p levels are increased [30].

Both KSRP and FUBP1 proteins have a conserved architecture of 4 tandem KH domains to interact with RNA/DNA [34]. However, KSRP mainly interacts with RNA via its third KH domain (KH3) and substituting the key GXXG residues of KH domain with GDDG significantly decreased the interaction of KSRP to RNA [32]. Therefore, to test whether FUBP1 interacts with pre-miR-155 through its KH3 domain, we generated recombinant WT and KH3 domain GDDG mutants for FUBP1 and KSRP (**Figure 6a**). We then measured the interaction of these recombinant proteins to pre-miR-155 using biolayer interferometry (BLI). **Figures 6b and 6c** shows that both KSRP WT and FUBP1 WT interact with pre-miR-155, but the KH3 GDDG mutants of KSRP and FUBP1 do not.

Preprints (www.preprints.org) | NOT PEER-REVIEWED | Posted: 15 November 2021 doi:10.20944/preprints202111.0272.v1

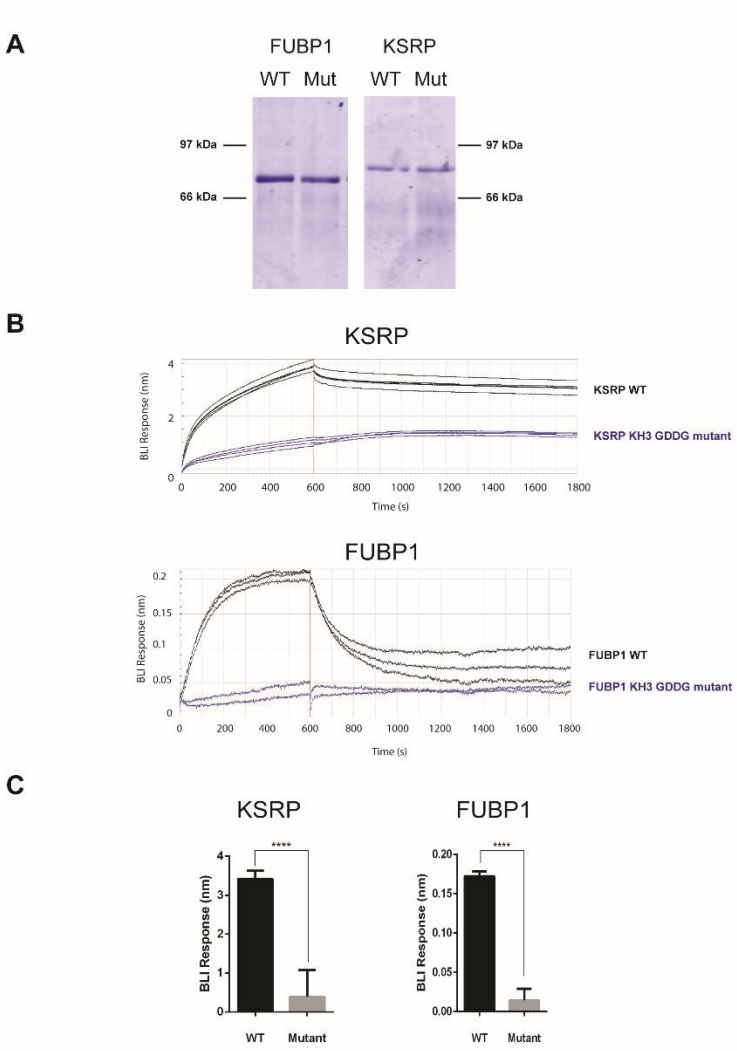

Figure 6. KH3 domain of KSRP and FUBP1 are essential to interact with pre-miR-155

KSRP/FUBP1 WT or KSRP/FUBP1 KH3 GDDG mutant proteins were expressed and purified as described in the material and methods. (a) The purity of the purified protein was assessed by Coomassie Blue staining of the gel. (b) BLI biosensors loaded with biotinylated pre-miR-155 were dipped in wells containing KSRP WT, KSRP KH3 GDDG mutant, FUBP1 WT, FUBP1 KH3 GDDG mutant proteins for 10 minutes, followed by a dissociation step in the assay buffer for 20 minutes. (c) Data plotted to represent the BLI response of indicated proteins with biotinylated pre-miR-155. Unpaired Student's t-test determined the comparison between the WT and KH3 GDDG mutant. **** $p < 0.0001$, *** $p < 0.001$.

3. Discussion

Our data show that knocking down either FUBP1 or CELF2 enhances LPS-induced expression of pri-miR-155 and pre-miR-155, suggesting that these RNA binding proteins can regulate the levels of these RNAs. However, both FUBP1 and CELF2 regulate the expression of miR-155-5p and miR-155-3p beyond the effect of these proteins on pri-miR-155 and pre-miR-155 (summarized in **Figure 7**). CELF2 inhibits miR-155-p while FUBP1 enhances miR-155-3p expression in LPS-stimulated cells. Furthermore, IL10 inhibition of miR-155-3p requires FUBP1, STAT3, and SHIP1, whereas inhibition of miR-155-5p required only CELF2 and STAT3. Finally, the point mutations in KH3 domain of FUBP1, analogous to the KH3 domain in KSRP reported to bind pre-miR-155 [35], abrogated FUBP1's ability to bind pre-miR-155.

Preprints (www.preprints.org) | NOT PEER-REVIEWED | Posted: 15 November 2021 doi:10.20944/preprints202111.0272.v1

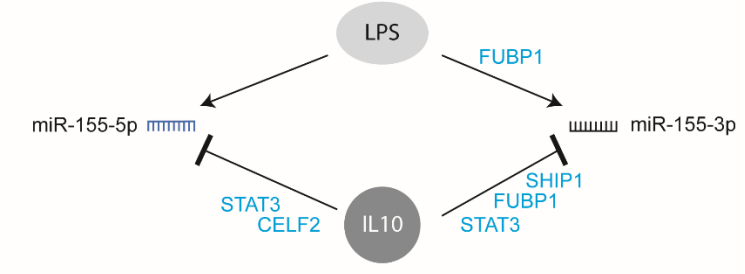

Figure 7. Schematic representation of miR-155 regulation

Schematic diagram representing the regulation of miR-155-5p and miR-155-3p expression in response to LPS and IL10. Note this diagram illustrates only FUBP1, CELF2, SHIP1, and STAT3 control of miR-155-5p/miR-155-3p, not due to the effects of these proteins on pri-miR-155 and pre-miR-155 expression.

In addition to FUBP1's control of pri-miR-155 and pre-miR-155, FUBP1 also regulates miR-155-3p levels (**Figure 2b**). The FUBP1 knockdown studies suggest that FUBP1 participates in LPS stimulation and IL10 inhibition of miR-155-3p. However, FUBP1 knockdown appears to have no further effect on miR-155-5p independent of its impact on pri-miR-155 and pre-miR-155. IL10 inhibition of miR-155-5p is impaired in CELF2 KD cells, as we have previously described [25]. However, our current data suggest this is partly due to the requirement for CELF2 for IL10 inhibition of pre-miR-155 expression.

IL10 signaling downstream of the IL10R involves both STAT3 and SHIP1:STAT3 pathways [14]. Therefore, we examined the STAT3 and SHIP1 dependency of IL10 regulation of pri-miR-155, pre-miR-155, miR-155-5p and miR-155-3p. We found that IL10 required only STAT3 to inhibit pri-miR-155, pre-miR-155 and miR-155-5p, and miR-155-3p (**Figure 4b**). The STAT3-only requirement for IL10 inhibition of miR-155-5p contrasts with our previous observation that IL10 inhibition of miR-155-5p expression required both SHIP1 and STAT3 [18]. In that study, we used perimacs allowed to rest in culture overnight before the stimulations. An overnight rest period better lets us observe the responses of the cells independent of the environment those cells might have experienced in the mouse. For example, the SHIP1 KO mouse has elevated specific cytokines in its circulation [36]. However, we now use perimacs within 2 hours of extraction from the mouse, so the cells more resemble their native state in the mouse. With these 2-hour rested perimacs, we found: (i) basal levels of miR-155-5p and miR-155-3p are higher in the SHIP1 KO than SHIP1 WT cells, and (ii) LPS induction of miR-155-5p and miR-155-3p is reduced in the KO as compared to the WT cells. The increased basal miR-155 expression may reflect the lack of SHIP1 in these cells since SHIP1 is a negative regulator of miR-155 expression [37]. On the other hand, the reduced miR-155-5p and miR-155-3p levels induced by LPS in the SHIP1 KO cells may be due to network-dosage compensatory mechanisms [38] developed in the cell to blunt stimulation-dependent elevation of miR-155 levels above the basal level.

With these caveats in mind for interpretation of the data from the SHIP1 KO cells, we examined the ability of IL10 to inhibit the LPS-induction of miR-155-5p and miR-155-3p in SHIP1 WT and SHIP1 KO cells (**Figure 5b**, normalized to each cell's own LPS-stimulated samples). As **Figure 5b** shows, IL10 can inhibit LPS-induced miR-155-5p in both SHIP1 WT and KO cells, but SHIP1 deficiency impairs Il10 inhibition of miR-155-3p. These data suggest the IL10 control of miR-155-5p requires only STAT3 but control of miR-155-3p requires both SHIP1 and FUBP1 (summarized in **Figure 7**).

Most investigators have focused on studying miR-155-5p because it is the more abundant miR-155 strand [7,19,39,40]. Simmonds *et al.* were the first to report that LPS also induces miR-155-3p human macrophages; miR-155-3p expression peaked earlier (around

 doi:10.20944/preprints202111.0272.v1

2 hours) and disappeared by 24 hours [26]. In contrast, miR-155-5p levels do not rise until about 2-4 hours and remain detectable at 24 hours [26]. We also found in WT mouse macrophages that LPS-induced miR-155-3p expression increases more quickly than miR-155-5p (**Figure 4c** and **Figure 5c**). In the C57BL/6 mouse (STAT3 WT), the peak of miR-155-3p occurs at 2 hours. In the BALB/c mouse (SHIP1 WT), miR-155-3p can be detected at 2 hours, remaining high at 4 hours. As in human macrophages, miR-155-5p expression is delayed with respect to miR-155-3p. miR-155-5p is detected only by 4 hours in the BALB/c (SHIP1 WT) mice (**Figure 5c)**. In the C57BL/6 (STAT3 WT) mice, miR-155-5p expression was also delayed compared to miR-155-3p (**Figure 4c)**. Thus, despite the difference in the magnitude of miR-155-5p expression at 2 hours in the two strains, the data still support a change in expression from miR-155-3p to miR-155-5p at around 2 hours.

We had previously examined the kinetics of IL10 inhibition of LPS-induced expression of TNFα [14]. We showed that the early (within 2 hours) response required a SHIP1:STAT3 complex, while the late phase (>2 hours) only needed STAT3. In the current study, we found that miR-155-3p becomes expressed earlier than miR-155-5p, and inhibition of miR-155-3p requires SHIP1 and STAT3, while inhibition of miR-155-5p requires only STAT3 (**Figure 7**). These observations suggest that IL10 inhibition of miR-155-3p may be necessary for IL10 inhibition of the early (SHIP1/STAT3 dependent) phase of TNFα production. In contrast, miR-155-5p participates in inhibition of the late (STAT3 dependent) phase of TNFα expression. However, the mechanism by which STAT3 or SHIP1:STAT3 complexes control miR-155-5p and miR-155-3p remains to be determined. One possibility is that both lead to proteins' expression that participates in the control of pre-miR-155 processing. In fact, since the absence of STAT3 results in IL10 *enhancing* rather than *reducing* LPS-induced miR-155-5p and miR-155-3p levels, we predict these STAT3-induced proteins may suppress pre-miR-155 processing.

FUBP1 has not been previously described to participate in miRNA processing. Ruggiero *et al.* reported that KSRP binds pre-miR-155 and is required to mature pre-miR-155 to miR-155-5p [28]. The effect of KSRP KD [30] (decrease LPS-induced miR-155-5p and increase miR-155-3p) is opposite to that of FUBP1 KD (**Figure 2c,** increase LPS-induced miR-155-5p and decrease LPS-induced miR-155-3p), suggesting the role of FUBP1 and KSRP as miR-155-3p and miR-155-5p enhancers, respectively (summarized in **Figure 8a**). Our work indicates the KH3 domain of FUBP1 participates in binding to pre-miR-155, analogous to the requirement of the KSRP KH3 domain for miR-155-5p binding [28]. The KH3 domain of FUBP1 and KSRP share 79% sequence homology (**Figure 8b**). Thus KSRP and FUBP1 may recognize the same or similar sequences in pre-miR-155. The consensus recognition motif for the KSRP KH3 domain (GGGG) [35] and FUBP1 KH3 domain (UUGUG) [41] both appear at the 3' end of the miR-155-5p sequence of pre-miR-155 (**Figure 8c**). Future studies will examine whether FUBP1 and KSRP compete to interact with pre-miR-155 in this region.

Preprints (www.preprints.org) | NOT PEER-REVIEWED | Posted: 15 November 2021 doi:10.20944/preprints202111.0272.v1

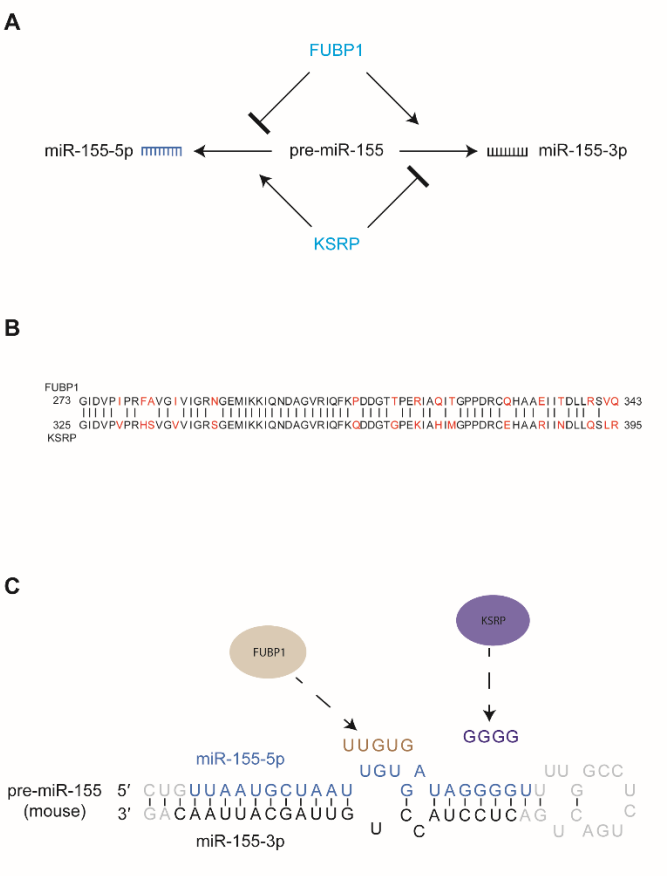

Figure 8. Schematic representation of FUBP1/KSRP regulation, homology, and interaction.

(a) Interplay between FUBP1 and KSRP in the regulation of miR-155-5p and miR-155-3p. (b) The sequence alignment of the KH3 domain of FUBP1 and KSRP protein. Sequences in black and red indicate matching and mismatching sequences, respectively. (c) Schematic diagram showing the predicted interaction site of FUBP1 and KSRP to pre-miR-155. The bases of pre-miR-155 are in gray; blue bases show the miR-155-5p sequence, and black bases indicate the miR-155-3p sequence.

KSRP processes and controls the expression of miRNAs (miR-145, miR-150, let-7a) [29,42,43] other than miR-155, and the proposed mechanism involves recruitment of proteins such as Drosha, DGCR8, and Dicer [29]. Interestingly, all the miRNAs controlled by KSRP have the 5p strand as the dominantly expressed strand (guide strand) and the 3p strand as the passenger strand [44-46]. Thus, KSRP may be participating in strand selection by bringing specific proteins into the Dicer complex that enhances the thermodynamic stability [47] of the 5p strand binding to the Dicer protein. The increased strength may result in selective processing of the 5p strand into the mature guide strand. Conversely, the association of FUBP1 with pre-miR-155 may bring in proteins that favor the processing of the 3p strand.

We found that FUBP1 is required for both LPS *induction* of miR-155-3p and IL10 dependent *inhibition* of miR-155-3p expression (**Figure 7**). However, although the amount of FUBP1 protein associated with pre-miR-155 increases in LPS-stimulated cells (compared to unstimulated cells), the amount of FUBP1 protein observed in the pre-miR-155 pull-down from LPS or LPS + IL10 treated cells are about the same (**Figure 1**). Similar amounts of FUBP1 bound suggests the difference in the outcome of FUBP1-dependent, LPS vs. IL10 action on miR-155-3p must be mediated by a difference other than FUBP1 simply binding to pre-miR-155. Post-translational modification or association with other proteins might regulate FUPB1 in LPS vs. LPS + IL10 treated cells.

Preprints (www.preprints.org) | NOT PEER-REVIEWED | Posted: 15 November 2021 doi:10.20944/preprints202111.0272.v1

Future studies involve characterizing the mechanisms of FUBP1 and CELF2 control of pri-miR-155 and pre-miR-155 levels, FUBP1 regulation of miR-155-5p vs. miR-155-3p expression, and the possible competition of FUBP1 with KSRP. It will also be essential to identify the 3p and 5p target genes relevant to LPS and IL10 control of macrophage function. These investigations will also provide insight into the regulation of other miRNAs' expression, especially those also described to be regulated by KSRP [29,42,43,48].

4. Materials and Methods

4.1. Mouse colonies

SHIP1 WT or SHIP1 KO (in the BALB/c background) mice were provided by Dr. Gerald Krystal (BC Cancer Research Centre, Vancouver, BC). STAT3 WT and KO mice (in the C57BL/6 background) were generated as described [14]. All mice were maintained in accordance with the animal care protocols approved by the University of British Columbia Animal Care Committee.

4.2. Cell lines

The murine cell line RAW264.7 (ATCC TIB-71) was maintained in Roswell Park Memorial Institute 1640 medium (RPMI-1640, SH30027, HyClone, Logan, UT) supplemented with 9% fetal bovine serum (FBS, SH30396, HyClone, Logan, UT). FUBP1 KD RAW264.7 cells were generated by transduction of RAW 264.7 expressing iCas9 (called RAW264.7 parental cells) as described below. The generation of CELF2 KD RAW264.7 cells was described in Yoon *et al.* [25].

4.3. Construction of the FUBP1-pLX-sgRNA targeting vector

The FUBP1 sgRNA targeting sequence (5' GCTAAATCCGACCATCCCATC) was designed using the CRISPR Gold online tool [51]. Oligonucleotides corresponding to this sequence were cloned into the pLX-sgRNA vector, using overlap-extension PCR as described [25]. The pLX-sgRNA vector with target-specific insert was transformed into chemically competent Stbl3 *E. coli* cells and colonies selected using ampicillin. The resulting FUBP1-pLX-sgRNA construct was confirmed by sequencing.

4.4. Generation of RAW 264.7 cells expressing FUBP1-pLX-sgRNA

The FUBP1-pLX-sgRNA vector was transduced into RAW264.7 cells expressing iCas9 (called RAW264.7 parental cells) [25] using lentiviruses. Lentiviruses harboring FUBP1-pLX-sgRNA were prepared by co-transfecting FUBP1-pLX-sgRNA vector into HEK293T (ATCC CRL-3216) cells with the packaging plasmid R8.9 and VSVG. 24 hours after transfection, the supernatant was collected and incubated with RAW264.7 parental cells in the presence of 8 μg/mL protamine sulfate. Cells transduced with FUBP1-pLX-sgRNA viruses were selected using 10 μg/mL blasticidin2 μg/mL doxycycline was added to the culture media for up to 48 hours to induce the expression of Cas9 and knockdown of FUBP1.

4.5. RNA-oligonucleotide transfection and RNA pull-down assay

RAW264.7 cells (ATCC TIB-71) were seeded at 8.4 x 10^6 cells per 10 cm dish a day before the transfection. Biotinylated pre-miR-155 oligonucleotides (Biotin-UAAUUGUGAUAGGGGUUU UGGCCUCUGACUGACUCCUACCUGUUA) was obtained from Invitrogen Life Technologies (ThermoFisher Scientific, Nepean, ON). RNA oligonucleotides and Lipofectamine-3000 (L3000-015, ThermoFisher Scientific, Nepean, ON) were prepared in Opti-MEM (31985, ThermoFisher Scientific, Nepean, ON) separately and was mixed at 1:1 (v/v) ratio, incubated at room temperature for 20 minutes to allow the formation of Lipofectamine-oligonucleotide complexes. 1 μg of RNA-oligonucleotide to 1.125 μL of Lipofectamine-3000 was used. After incubation, the RNA-Lipofectamine solu-

Preprints (www.preprints.org) | NOT PEER-REVIEWED | Posted: 15 November 2021 doi:10.20944/preprints202111.0272.v1

tion was diluted ten-fold with 9% FBS/RPMI-1640 and added to cells. The cells were incubated with the transfection solution in a chamber at 37°C supplemented with 5% CO_2. After 6 hours, the solution was replaced with 9% FBS/RPMI-1640, and cells were allowed to recover overnight

Following the 9% FBS/RPMI-1640 overnight incubation, the transfected RAW264.7 cells were stimulated with 1 ng/mL LPS (*Escherichia coli* serotype 0111:B4; Millipore-Sigma, Oakville, ON) ± 50 ng/mL IL10 for the indicated length of time in a chamber at 37°C supplemented with 5% CO_2. Following stimulation, the media was removed, and cells were chilled with cold (4°C) phosphate-buffered saline (PBS, SH30256, ThermoFisher Scientific, Nepean, ON) for 2 minutes. Next, the PBS was removed and the cells lysed by the addition of protein solubilization buffer (PSB, 50 mM HEPES, 100 mM NaF, 10 mM NaPPi, 2 mM $NaVO_4$, 2 mM $NaMoO_4$, 4 mM EDTA, 0.125% Triton X-100, protease inhibitor cocktail (11836145001, Millipore-Sigma, Oakville, ON), and 0.5 mM Tris(2-carboxyethyl)phosphine (TCEP, M115, Soltec Ventures, Beverly, MA)). Cell lysates were collected with a cell scraper and gently agitated at 4°C for 30 minutes. Insoluble material was removed by centrifugation at 12,000 RPM for 20 minutes at 4°C.

Clarified cell lysates were added to streptavidin magnetic beads (1164786001, Millipore-Sigma, Oakville, ON) in 1.5 mL microfuge tubes and incubated for 90 minutes at 4°C on a nutator. The tubes were then briefly centrifuged at 5,000 RPM, and magnetic beads were immobilized using a magnetic tube stand (12321D, ThermoFisher Scientific, Nepean, ON). Lysates were removed, and the beads were resuspended in the wash buffer (0.1% Tween-20 containing PSB) and rocked for 5 minutes at 4°C on a nutator. The washing was repeated 3 times. The proteins were eluted by boiling 2x SDS-PAGE sample buffer (0.125 M Tris, pH 6.8, 5% 2-mercaptoethanol, bromophenol blue, 13.5% glycerol, 4.5 % SDS) for immunoblot analysis.

4.6. Immunoblot analysis

Proteins were separated by 10% SDS-PAGE, followed by electroblotting onto polyvinylidene fluoride (PVDF) membrane (IPFL00010, Millipore-Sigma, Oakville, ON). The membranes were blocked in 3% bovine serum albumin (BSA), then probed with the following primary antibodies overnight: 1:1000 KSRP (ab140648, Abcam, Toronto, ON), 0.1 μg/mL GAPDH (G9545, Millipore-Sigma, Oakville, ON), and 1 μg/mL FUBP1 (Sc-136137, Santa Cruz, Dallas, TX). The membranes were washed three times in Tris-buffered saline containing 0.05% Tween-20 (TBST), incubated with either Alexa Fluor 660 anti-mouse IgG (A21055) or Alexa Fluor 680 anti-rabbit IgG (A21109, Invitrogen , Burlington, ON), and imaged using a LI-COR Odyssey Imager.

4.7. Isolation of and stimulation of mouse peritoneal macrophages

Primary peritoneal macrophages (perimacs) were isolated from mice by peritoneal lavage with 3 mL of sterile PBS. Perimacs were seeded at 2.0 x 10^6 cells per well in a 6-well tissue culture plate or 1.18 x 10^6 cells per well in a 24-well tissue culture plate in Iscove's Modified Dulbecco's Medium (IMDM, SH30228, HyClone, Logan, UT) supplemented with 10% FCS. Cells were allowed to adhere for 2 hours, rinsed with room temperature PBS to remove non-adhered cells, and fresh media added. The media was changed after 1 hour, and the cells were stimulated with 1 ng/mL LPS ± 1 ng/mL IL10 for 1, 2, or 4 hours. Triplicate wells were used for each stimulation condition.

4.8. RNA extraction and qPCR

Total RNA was extracted using Tri-Reagent (T9424, Millipore-Sigma, Oakville, ON) according to the manufacturer's instructions. 1-3 μg of RNA was treated with RNase-free DNase I (04716728001, Millipore-Sigma, Oakville, ON) for 20 minutes at 37°C, followed by the addition of 0.1 M EDTA to a final concentration of 8 mM to inactivate DNase I.

For measurement of miR-155-5p, miR-155-3p, and small nucleolar RNA MBII-202 (snoRNA202) levels, 20 ng of DNase I treated RNA was used to generate cDNAs using the miRNA TaqMan Reverse Transcription Kit (4366597, ThermoFisher Scientific, Ne-

Preprints (www.preprints.org) | NOT PEER-REVIEWED | Posted: 15 November 2021 doi:10.20944/preprints202111.0272.v1

pean, ON), Multiscribe™ reverse transcriptase (4319983, ThermoFisher Scientific, Nepean, ON), and miR-155-5p (002571), miR-155-3p (464539_mat) or snoRNA202 (001232, ThermoFisher Scientific, Nepean, ON) primers according to the manufacturer's instructions. qPCR quantification of miR-155-5p and miR-155-3p and snoRNA202 cDNA was performed using the TaqMan fast advanced master mix (4444557, ThermoFisher Scientific, Nepean, ON) and the appropriate TaqMan probes on a StepOne Plus™ instrument (4376582, Invitrogen, Burlington, ON). miRNA levels were analyzed using the comparative CT method with snoRNA202 as the normalization control.

For measurement of pri-miR-155, pre-miR-155, and GAPDH, 200 ng of DNase I treated RNA were reverse transcribed using SuperScript™ IV reverse transcriptase and random hexamers (18090050, ThermoFisher Scientific, Nepean, ON). qPCR quantification of pri-miR-155, pre-miR-155, and GAPDH were achieved with primers for pri-miR-155, pre-miR-155, and GAPDH in conjunction with the SYBR Green master mix (100029284, ThermoFisher Scientific, Nepean, ON). RNA levels were analyzed using the comparative CT method with GAPDH as the normalization control.

4.9. Molecular cloning of FUBP1 and KSRP

The open reading frame (ORF) of mouse FUBP1 and KSRP was obtained by PCR on cDNA generated from RNA isolated from SHIP1 WT perimacs. The FUBP1/KSRP ORF was inserted into the Gateway entry vector (pENTR1A, Invitrogen, Burlington, ON) via restriction digest and ligation. The products were transformed into DH5α *E. coli* chemically competent cells, and colonies were selected using 50 μg/mL of kanamycin. The sequences of the FUBP1/KSRP pENTR1A vectors were confirmed by sequencing. The GXXG sequences in the third KH domain of FUBP1 and KSRP were mutated to the GDDG sequence using site-directed mutagenesis. Briefly, PCR with non-overlapping primers (5' phosphorylated forward primer with desired mutation and non-overlapping reverse primer) were used to generate FUBP1/KSRP daughter plasmids containing the desired mutation. The resulting PCR product was extracted with phenol-chloroform, treated with Dpn I to remove the parental vector, daughter plasmids ligated with T4 ligase, and transformed into DH5α chemically competent cells. The FUBP1/KSRP WT and KH3 GDDG mutant pENTR1A vectors were transferred to lentiviral vector FUGWBW using Gateway LR reactions as we have described [14].

4.10. Recombinant FUPB1 and KSRP Protein Expression

HEK293T cells were transfected with FUBWBW vectors encoding FUBP1/KSRP WT or KH3 GDDG mutant proteins. After transfection (48 hours), the cells were lysed with the lysis buffer (20 mM Tris-HCl, pH 7.4, 150 mM NaCl, 5 mM imidazole, 1% NP-40, protease inhibitor cocktail, and 10 mM TCEP). The lysates were incubated for 45 minutes at 4°C on a nutator, then centrifuged at 12000 rpm for 20 minutes, and the supernatants were transferred to tubes containing cobalt affinity beads (TALON metal affinity resin, #635504, Takara Bio, Mountain View, CA). The cell lysates were incubated with the beads for 2 hours, and the beads were washed three times with wash buffer (20 mM Tris-HCl, pH 7.4, 150 mM NaCl, 5 mM Imidazole, 0.1% NP-40, 0.5 mM TCEP) before eluting with the elution buffer (20 mM Tris-HCl, pH 7.4, 150 mM NaCl, 150 mM imidazole, 0.5 mM TCEP, and 0.02% Tween-20).

4.11. Measurement of TNFα production

Cells were seeded at 2.0 x 10^4 cells per well in a 96-well tissue culture plate and allowed to adhere overnight. The media was changed the next day 1 hour before stimulation. Cells were stimulated with 1 ng/mL of LPS ± indicated concentration of IL10 for 1 hour. Triplicate wells were used for each stimulation condition. The supernatant was collected, and secreted TNFα protein levels were measured using a BD OptEIA Mouse TNFα Enzyme-Linked Immunosorbent Assay (ELISA) kit (558534, BD Biosciences, Mississauga, ON).

4.12. Biolayer interferometry(BLI)

The binding affinity between the FUBP1 or KSRP proteins to pre-miR-155 was examined using biolayer interferometry with super-streptavidin (SSA) biosensor tips (18-5057, ForteBio, Fremont, CA). SSA biosensor tips were hydrated in BLI assay buffer (20 mM Tris-HCl, pH 7.4, 150 mM NaCl, 0.5 mM TCEP, 0.2% Tween-20) prior to coating with biotinylated pre-miR-155 and blocking with 0.1% BSA. The kinetic measurements were done at 30°C with an orbital flow of 1000 rpm. A 60 second baseline was established using BLI assay buffer. The pre-miR-155 coated biosensors were then dipped into wells containing KSRP or FUBP1 protein and association monitored for 600 seconds. The sensors were then transferred to wells containing only BLI assay buffer, and protein dissociation was monitored for 600 seconds. The raw data were analyzed using the Octet Red Data Analysis software (ver. 8.2).

4.13. Statistical analysis

Band intensities were quantified in immunoblots using LI-COR Odyssey imaging system and Image Studio™ Lite software (LI-COR Biosciences, Lincoln, NE). Graph-Pad Prism 6 (GraphPad Software Inc., La Jolla, CA) was used to perform all statistical analyses. Statistical details can be found in figure legends. Values are presented as means ± standard deviations. Unpaired Student's *t*-tests were used where appropriate to generate two-tailed P values. Two-way ANOVA was performed where required with appropriate multiple comparisons tests. The differences were considered significant when $p \leq 0.05$.

4.14. Ethical statement

The perimacs were derived from mice in accordance with the animal care protocol (A21-0203) approved by the University of British Columbia Animal Care Committee. The cell culture experiments are done in accordance with UBC Biosafety requirements (B16-0206).

Author Contributions: Conceptualization, J.Y., and A.M.; methodology, J.Y.; validation, J.Y., T.C. and A.M.; formal analysis, J.Y.; investigation, J.Y. , A.W., and A.M.;. resources, J.Y., and T.C.; data curation, J.Y., and A.W..; writing—original draft preparation, J.Y., and A.W.; writing—review and editing, J.Y., T.C. and A.M.; visualization, J.Y.; supervision, A.M.; project administration, T.C., and A.M.; funding acquisition, A.M. All authors have read and agreed to the published version of the manuscript.

Funding: This research was supported by operating grants from the Canadian Institutes of Health Research (MOP-133415) and the Natural Science of Engineering Research Council (RGPIN-2014-05662).

Institutional Review Board Statement: The perimacs were derived from mice in accordance with the animal care protocol (A21-0203) approved by the University of British Columbia Animal Care Committee.

Acknowledgments: We would like to thank Dr. Nada Lallous from Vancouver Prostate Centre for providing help with the BLI experiments and Dr. Gerald Krystal for the SHIP1 WT and KO mice. We also thank Mike K. Wu for advice on the RNA pull-down experiments.

Conflicts of Interest: The authors declare no conflict of interest. The funders had no role in the design of the study; in the collection, analyses, or interpretation of data; in the writing of the manuscript, or in the decision to publish the results.

References

1.

1. Lee, Y.; Jeon, K.; Lee, J.T.; Kim, S.; Kim, V.N. MicroRNA maturation: stepwise processing and subcellular localization. *EMBO J* **2002**, *21*, 4663-4670, doi:10.1093/emboj/cdf476.

2. Lee, R.C.; Feinbaum, R.L.; Ambros, V. The C. elegans heterochronic gene lin-4 encodes small RNAs with antisense complementarity to lin-14. *Cell* **1993**, *75*, 843-854, doi:10.1016/0092-8674(93)90529-y.
3. Bartel, D.P. MicroRNAs: genomics, biogenesis, mechanism, and function. *Cell* **2004**, *116*, 281-297, doi:10.1016/s0092-8674(04)00045-5.
4. Parameswaran, N.; Patial, S. Tumor necrosis factor-α signaling in macrophages. *Crit Rev Eukaryot Gene Expr* **2010**, *20*, 87-103.
5. Zhang, Y.; Li, Y.K. MicroRNAs in the regulation of immune response against infections. *J Zhejiang Univ Sci B* **2013**, *14*, 1-7, doi:10.1631/jzus.B1200292.
6. Rauh, M.J.; Sly, L.M.; Kalesnikoff, J.; Hughes, M.R.; Cao, L.P.; Lam, V.; Krystal, G. The role of SHIP1 in macrophage programming and activation. *Biochem Soc Trans* **2004**, *32*, 785-788, doi:10.1042/BST0320785.
7. O'Connell, R.M.; Taganov, K.D.; Boldin, M.P.; Cheng, G.; Baltimore, D. MicroRNA-155 is induced during the macrophage inflammatory response. *Proc Natl Acad Sci U S A* **2007**, *104*, 1604-1609, doi:10.1073/pnas.0610731104.
8. Sonkoly, E.; Pivarcsi, A. Advances in microRNAs: implications for immunity and inflammatory diseases. *J Cell Mol Med* **2009**, *13*, 24-38, doi:10.1111/j.1582-4934.2008.00534.x.
9. Chandan, K.; Gupta, M.; Sarwat, M. Role of Host and Pathogen-Derived MicroRNAs in Immune Regulation During Infectious and Inflammatory Diseases. *Front Immunol* **2019**, *10*, 3081, doi:10.3389/fimmu.2019.03081.
10. Chen, L.; Deng, H.; Cui, H.; Fang, J.; Zuo, Z.; Deng, J.; Li, Y.; Wang, X.; Zhao, L. Inflammatory responses and inflammation-associated diseases in organs. *Oncotarget* **2018**, *9*, 7204-7218, doi:10.18632/oncotarget.23208.
11. Mantovani, A.; Allavena, P.; Sica, A.; Balkwill, F. Cancer-related inflammation. *Nature* **2008**, *454*, 436-444, doi:10.1038/nature07205.
12. Moore, K.W.; de Waal Malefyt, R.; Coffman, R.L.; O'Garra, A. Interleukin-10 and the interleukin-10 receptor. *Annu Rev Immunol* **2001**, *19*, 683-765, doi:10.1146/annurev.immunol.19.1.683.
13. Armstrong, L.; Jordan, N.; Millar, A. Interleukin 10 (IL-10) regulation of tumour necrosis factor alpha (TNF-alpha) from human alveolar macrophages and peripheral blood monocytes. *Thorax* **1996**, *51*, 143-149, doi:10.1136/thx.51.2.143.
14. Chamberlain, T.C.; Cheung, S.T.; Yoon, J.S.J.; Ming-Lum, A.; Gardill, B.R.; Shakibakho, S.; Dzananovic, E.; Ban, F.; Samiea, A.; Jawanda, K.; et al. Interleukin-10 and Small Molecule SHIP1 Allosteric Regulators Trigger Anti-inflammatory Effects through SHIP1/STAT3 Complexes. *iScience* **2020**, *23*, 101433, doi:10.1016/j.isci.2020.101433.
15. Murray, P.J. STAT3-mediated anti-inflammatory signalling. *Biochem Soc Trans* **2006**, *34*, 1028-1031, doi:10.1042/BST0341028.
16. Zhong, Z.; Wen, Z.; Darnell, J.E. Stat3: a STAT family member activated by tyrosine phosphorylation in response to epidermal growth factor and interleukin-6. *Science* **1994**, *264*, 95-98.
17. Chan, C.S.; Ming-Lum, A.; Golds, G.B.; Lee, S.J.; Anderson, R.J.; Mui, A.L. Interleukin-10 inhibits lipopolysaccharide-induced tumor necrosis factor-alpha translation through a SHIP1-dependent pathway. *J Biol Chem* **2012**, *287*, 38020-38027, doi:10.1074/jbc.M112.348599.
18. Cheung, S.T.; So, E.Y.; Chang, D.; Ming-Lum, A.; Mui, A.L. Interleukin-10 inhibits lipopolysaccharide induced miR-155 precursor stability and maturation. *PLoS One* **2013**, *8*, e71336, doi:10.1371/journal.pone.0071336.
19. McCoy, C.E.; Sheedy, F.J.; Qualls, J.E.; Doyle, S.L.; Quinn, S.R.; Murray, P.J.; O'Neill, L.A. IL-10 inhibits miR-155 induction by toll-like receptors. *J Biol Chem* **2010**, *285*, 20492-20498, doi:10.1074/jbc.M110.102111.
20. El Kasmi, K.C.; Holst, J.; Coffre, M.; Mielke, L.; de Pauw, A.; Lhocine, N.; Smith, A.M.; Rutschman, R.; Kaushal, D.; Shen, Y.; et al. General nature of the STAT3-activated anti-inflammatory response. *J Immunol* **2006**, *177*, 7880-7888.
21. Mahesh, G.; Biswas, R. MicroRNA-155: A Master Regulator of Inflammation. *J Interferon Cytokine Res* **2019**, *39*, 321-330, doi:10.1089/jir.2018.0155.
22. Elton, T.S.; Selemon, H.; Elton, S.M.; Parinandi, N.L. Regulation of the MIR155 host gene in physiological and pathological processes. *Gene* **2013**, *532*, 1-12, doi:10.1016/j.gene.2012.12.009.

23. Meijer, H.A.; Smith, E.M.; Bushell, M. Regulation of miRNA strand selection: follow the leader? *Biochem Soc Trans* **2014**, *42*, 1135-1140, doi:10.1042/BST20140142.
24. Kehl, T.; Backes, C.; Kern, F.; Fehlmann, T.; Ludwig, N.; Meese, E.; Lenhof, H.P.; Keller, A. About miRNAs, miRNA seeds, target genes and target pathways. *Oncotarget* **2017**, *8*, 107167-107175, doi:10.18632/oncotarget.22363.
25. Yoon, J.S.J.; Wu, M.K.; Zhu, T.H.; Zhao, H.; Cheung, S.T.; Chamberlain, T.C.; Mui, A.L. Interleukin-10 control of pre-miR155 maturation involves CELF2. *PLoS One* **2020**, *15*, e0231639, doi:10.1371/journal.pone.0231639.
26. Simmonds, R.E. Transient up-regulation of miR-155-3p by lipopolysaccharide in primary human monocyte-derived macrophages results in RISC incorporation but does not alter TNF expression. *Wellcome Open Res* **2019**, *4*, 43, doi:10.12688/wellcomeopenres.15065.2.
27. Li, H.; Wang, Z.; Zhou, X.; Cheng, Y.; Xie, Z.; Manley, J.L.; Feng, Y. Far upstream element-binding protein 1 and RNA secondary structure both mediate second-step splicing repression. *Proc Natl Acad Sci U S A* **2013**, *110*, E2687-2695, doi:10.1073/pnas.1310607110.
28. Ruggiero, T.; Trabucchi, M.; De Santa, F.; Zupo, S.; Harfe, B.D.; McManus, M.T.; Rosenfeld, M.G.; Briata, P.; Gherzi, R. LPS induces KH-type splicing regulatory protein-dependent processing of microRNA-155 precursors in macrophages. *FASEB J* **2009**, *23*, 2898-2908, doi:10.1096/fj.09-131342.
29. Trabucchi, M.; Briata, P.; Garcia-Mayoral, M.; Haase, A.D.; Filipowicz, W.; Ramos, A.; Gherzi, R.; Rosenfeld, M.G. The RNA-binding protein KSRP promotes the biogenesis of a subset of microRNAs. *Nature* **2009**, *459*, 1010-1014, doi:10.1038/nature08025.
30. Zhou, H.; Huang, X.; Cui, H.; Luo, X.; Tang, Y.; Chen, S.; Wu, L.; Shen, N. miR-155 and its star-form partner miR-155* cooperatively regulate type I interferon production by human plasmacytoid dendritic cells. *Blood* **2010**, *116*, 5885-5894, doi:10.1182/blood-2010-04-280156.
31. King, P.H.; Chen, C.Y. Role of KSRP in control of type I interferon and cytokine expression. *J Interferon Cytokine Res* **2014**, *34*, 267-274, doi:10.1089/jir.2013.0143.
32. Hollingworth, D.; Candel, A.M.; Nicastro, G.; Martin, S.R.; Briata, P.; Gherzi, R.; Ramos, A. KH domains with impaired nucleic acid binding as a tool for functional analysis. *Nucleic Acids Res* **2012**, *40*, 6873-6886, doi:10.1093/nar/gks368.
33. Medley, J.C.; Panzade, G.; Zinovyeva, A.Y. microRNA strand selection: Unwinding the rules. *Wiley Interdiscip Rev RNA* **2021**, *12*, e1627, doi:10.1002/wrna.1627.
34. Davis-Smyth, T.; Duncan, R.C.; Zheng, T.; Michelotti, G.; Levens, D. The far upstream element-binding proteins comprise an ancient family of single-strand DNA-binding transactivators. *J Biol Chem* **1996**, *271*, 31679-31687, doi:10.1074/jbc.271.49.31679.
35. García-Mayoral, M.F.; Díaz-Moreno, I.; Hollingworth, D.; Ramos, A. The sequence selectivity of KSRP explains its flexibility in the recognition of the RNA targets. *Nucleic Acids Res* **2008**, *36*, 5290-5296, doi:10.1093/nar/gkn509.
36. Kuroda, E.; Antignano, F.; Ho, V.W.; Hughes, M.R.; Ruschmann, J.; Lam, V.; Kawakami, T.; Kerr, W.G.; McNagny, K.M.; Sly, L.M.; et al. SHIP represses Th2 skewing by inhibiting IL-4 production from basophils. *J Immunol* **2011**, *186*, 323-332, doi:10.4049/jimmunol.1002778.
37. O'Connell, R.M.; Chaudhuri, A.A.; Rao, D.S.; Baltimore, D. Inositol phosphatase SHIP1 is a primary target of miR-155. *Proc Natl Acad Sci U S A* **2009**, *106*, 7113-7118, doi:0902636106 [pii]
10.1073/pnas.0902636106.
38. Ferro, E.; Enrico Bena, C.; Grigolon, S.; Bosia, C. From Endogenous to Synthetic microRNA-Mediated Regulatory Circuits: An Overview. *Cells* **2019**, *8*, doi:10.3390/cells8121540.
39. Faraoni, I.; Antonetti, F.R.; Cardone, J.; Bonmassar, E. miR-155 gene: a typical multifunctional microRNA. *Biochim Biophys Acta* **2009**, *1792*, 497-505, doi:10.1016/j.bbadis.2009.02.013.

40. Tili, E.; Croce, C.M.; Michaille, J.J. miR-155: on the crosstalk between inflammation and cancer. *Int Rev Immunol* **2009**, *28*, 264-284, doi:10.1080/08830180903093796.
41. Miro, J.; Laaref, A.M.; Rofidal, V.; Lagrafeuille, R.; Hem, S.; Thorel, D.; Méchin, D.; Mamchaoui, K.; Mouly, V.; Claustres, M.; et al. FUBP1: a new protagonist in splicing regulation of the DMD gene. *Nucleic Acids Res* **2015**, *43*, 2378-2389, doi:10.1093/nar/gkv086.
42. Lin, Y.Y.; Chou, C.F.; Giovarelli, M.; Briata, P.; Gherzi, R.; Chen, C.Y. KSRP and MicroRNA 145 are negative regulators of lipolysis in white adipose tissue. *Mol Cell Biol* **2014**, *34*, 2339-2349, doi:10.1128/MCB.00042-14.
43. Chou, C.F.; Lin, Y.Y.; Wang, H.K.; Zhu, X.; Giovarelli, M.; Briata, P.; Gherzi, R.; Garvey, W.T.; Chen, C.Y. KSRP ablation enhances brown fat gene program in white adipose tissue through reduced miR-150 expression. *Diabetes* **2014**, *63*, 2949-2961, doi:10.2337/db13-1901.
44. Okato, A.; Arai, T.; Kojima, S.; Koshizuka, K.; Osako, Y.; Idichi, T.; Kurozumi, A.; Goto, Y.; Kato, M.; Naya, Y.; et al. Dual strands of pre-miR-150 (miR-150-5p and miR-150-3p) act as antitumor miRNAs targeting SPOCK1 in naïve and castration-resistant prostate cancer. *Int J Oncol* **2017**, *51*, 245-256, doi:10.3892/ijo.2017.4008.
45. Roush, S.; Slack, F.J. The let-7 family of microRNAs. *Trends Cell Biol* **2008**, *18*, 505-516, doi:10.1016/j.tcb.2008.07.007.
46. Kenyon, J.D.; Sergeeva, O.; Somoza, R.A.; Li, M.; Caplan, A.I.; Khalil, A.M.; Lee, Z. Analysis of -5p and -3p Strands of miR-145 and miR-140 During Mesenchymal Stem Cell Chondrogenic Differentiation. *Tissue Eng Part A* **2019**, *25*, 80-90, doi:10.1089/ten.TEA.2017.0440.
47. Suzuki, H.I.; Katsura, A.; Yasuda, T.; Ueno, T.; Mano, H.; Sugimoto, K.; Miyazono, K. Small-RNA asymmetry is directly driven by mammalian Argonautes. *Nat Struct Mol Biol* **2015**, *22*, 512-521, doi:10.1038/nsmb.3050.
48. Michlewski, G.; Cáceres, J.F. Antagonistic role of hnRNP A1 and KSRP in the regulation of let-7a biogenesis. *Nat Struct Mol Biol* **2010**, *17*, 1011-1018, doi:10.1038/nsmb.1874.
49. Wang, T.; Wei, J.J.; Sabatini, D.M.; Lander, E.S. Genetic screens in human cells using the CRISPR-Cas9 system. *Science* **2014**, *343*, 80-84, doi:10.1126/science.1246981.
50. Cao, J.; Wu, L.; Zhang, S.M.; Lu, M.; Cheung, W.K.; Cai, W.; Gale, M.; Xu, Q.; Yan, Q. An easy and efficient inducible CRISPR/Cas9 platform with improved specificity for multiple gene targeting. *Nucleic Acids Res* **2016**, *44*, e149, doi:10.1093/nar/gkw660.
51. Chu, V.T.; Graf, R.; Wirtz, T.; Weber, T.; Favret, J.; Li, X.; Petsch, K.; Tran, N.T.; Sieweke, M.H.; Berek, C.; et al. Efficient CRISPR-mediated mutagenesis in primary immune cells using CrispRGold and a C57BL/6 Cas9 transgenic mouse line. *Proc Natl Acad Sci U S A* **2016**, *113*, 12514-12519, doi:10.1073/pnas.1613884113.

2.